Scientific Report

TRANSPARENT PROCESS

EMBO reports

Resistance of glia-like central and peripheral neural stem cells to genetically induced mitochondrial dysfunction—differential effects on neurogenesis

Blanca Díaz-Castro[1,†], Ricardo Pardal[1,2,3,†], Paula García-Flores[1,3], Verónica Sobrino[1], Rocío Durán[1], José I Piruat[1,**] & José López-Barneo[1,2,3,*]

Abstract

Mitochondria play a central role in stem cell homeostasis. Reversible switching between aerobic and anaerobic metabolism is critical for stem cell quiescence, multipotency, and differentiation, as well as for cell reprogramming. However, the effect of mitochondrial dysfunction on neural stem cell (NSC) function is unstudied. We have generated an animal model with homozygous deletion of the succinate dehydrogenase subunit D gene restricted to cells of glial fibrillary acidic protein lineage (hGFAP-SDHD mouse). Genetic mitochondrial damage did not alter the generation, maintenance, or multipotency of glia-like central NSCs. However, differentiation to neurons and oligodendrocytes (but not to astrocytes) was impaired and, hence, hGFAP-SDHD mice showed extensive brain atrophy. Peripheral neuronal populations were normal in hGFAP-SDHD mice, thus highlighting their non-glial (non hGFAP$^+$) lineage. An exception to this was the carotid body, an arterial chemoreceptor organ atrophied in hGFAP-SDHD mice. The carotid body contains glia-like adult stem cells, which, as for brain NSCs, are resistant to genetic mitochondrial damage.

Keywords carotid body stem cells; mitochondrial dysfunction; neural stem cells; peripheral versus central neurogenesis
Subject Categories Stem Cells; Neuroscience
DOI 10.15252/embr.201540982 | Received 7 July 2015 | Revised 20 August 2015 | Accepted 21 August 2015 | Published online 21 September 2015
EMBO Reports (2015) 16: 1511–1519

Introduction

Intermediary metabolism plays a critical role in stem cell maintenance and differentiation. Somatic stem cells in their niches are normally in a quiescent state and maintained under a predominantly anaerobic condition, which helps to preserve them from excessive production of reactive oxygen species and other stressors [1,2]. Indeed, hypoxia is believed to be an essential environmental factor for maintenance of the stemness in embryonic and adult stem cells [3,4]. Upregulation of hypoxia-inducible glycolytic genes is a hallmark of somatic stem cells [5,6] as well as embryonic and induced pluripotent stem cells (iPSCs) [7]. In contrast, oxidative phosphorylation appears to be necessary for hematopoietic stem cell (HSC) differentiation to mature cells [8]. An inverse metabolic switch (i.e., involving a change from aerobic to anaerobic metabolism) has also been reported to occur upon reprogramming of adult cells to iPSCs [7,9]. Although the role of mitochondria in pluripotency and differentiation is a topic at the forefront of stem cell research [2,7], the actual effect of *in vivo* mitochondrial dysfunction on stem cell survival and differentiation is poorly understood. This is particularly evident in the case of neural stem cells (NSCs), despite the fact that oxidative phosphorylation is critical for neuronal homeostasis, possibly more than for any other cell type.

Adult multipotent NSCs exist both in the central (CNS) and the peripheral (PNS) nervous system. During CNS development, radial glia, a cell type originated from the primordial neuroepithelium, serve as stem cells from which many neurons in cortical and subcortical areas as well as astrocytes and oligodendrocytes are derived [10,11]. A population of NSCs of astroglial lineage remains in the subventricular zone (SVZ) and the hippocampus of the adult mammalian brain, thereby supporting neurogenesis throughout life [11]. In contrast with the CNS, the PNS derives from a non-homogeneous population of neural crest progenitors that migrate throughout the embryo and give rise to neurons and peripheral glia during fetal and early postnatal life [12,13]. Multipotent neural crest progenitor cells in the PNS also persist in adult life, particularly in the enteric nervous system (ENS) [14,15] and in the carotid body (CB), a neural crest-derived peripheral chemoreceptor organ located at the carotid artery bifurcation that grows in response to hypoxia [16,17]. Whether CB stem cells and other peripheral adult NSCs

1 Instituto de Biomedicina de Sevilla (IBiS), Hospital Universitario Virgen del Rocío, CSIC, Universidad de Sevilla, Seville, Spain
2 Departamento de Fisiología Médica y Biofísica, Universidad de Sevilla, Sevilla, Spain
3 Centro de Investigación Biomédica en Red sobre Enfermedades Neurodegenerativas (CIBERNED), Madrid, Spain
*Corresponding author. Tel: +34 955 923007; E-mail: lbarneo@us.es
**Corresponding author. Tel: +34 955 923088; E-mail: jpiruat-ibis@us.es
†These authors contributed equally to this work

share a similar glial phenotype and metabolic properties with central neurogenic progenitors is not known.

We have generated a mouse model with conditional deletion of the gene encoding the membrane anchoring subunit D of succinate dehydrogenase restricted to cells expressing Cre recombinase under control of the human glial fibrillary acidic protein (hGFAP) promoter (hGFAP-SDHD mouse), which is active in mouse radial glia (see Materials and Methods). It is known that ablation of this mitochondrial complex II (MCII) gene in catecholaminergic cells compromises ATP synthesis and results in oxidative stress and neuronal loss in the brain and PNS [17,18]. This new animal model has permitted us to examine experimentally the resistance of neural stem cells to genetically induced mitochondrial dysfunction, which has remained untested so far. The experiments have also provided valuable information on the differential origin and properties of neural stem cells in the CNS and PNS, which might be relevant to their ability to support neurogenesis in adult life.

Results and Discussion

Genetic modification of mitochondrial function in embryonic radial glia alters neuronal maturation during brain development

Mutant (hGFAP-SDHD) mice were viable and did not exhibit any obvious alterations at birth. At postnatal day (P) 0, brains of mutant animals had similar appearance as those of control littermates, although dilation of ventricles was observed in some cases (Fig EV1). However, during the second week of life, hGFAP-SDHD mice exhibited a marked phenotype characterized by a lack of motor coordination, ataxia and decreased body size (Fig EV2A). Animals rapidly deteriorated and died between P16 and P18. At P15, the brains of GFAP-SDHD mice displayed notable malformations and were approximately 50% smaller than those of controls (Fig 1A). Anatomical and histological differences between brains of mutant mice and controls are illustrated in Fig 1B–M. Coronal sections stained with the neuronal marker NeuN at different rostro-caudal levels indicated marked atrophy of the cerebral cortex, particularly the dorso-lateral region, and a virtual absence of the hippocampus and cerebellum in hGFAP-SDHD mice with respect to controls, which at this age had already developed a normal adult brain. Detailed cytoarchitectonic or neuronal identification analyses were outside the scope of this work; however, the disappearance of cortical layers in the fronto-parietal region and atrophy of the corpus callosum were clearly evident histological hallmarks of hGFAP-SDHD mice (Fig 1B–E). In these animals, the regions normally occupied by the hippocampus and cerebellum contained only embryonic primordial rudiments of these structures (Fig 1F–M). The temporo-cortical areas, basal nuclei, and ventro-caudal brain (diencephalon and brain stem) appeared less affected (Fig 1B, C, F and G; see sagittal sections and details of structures at higher magnification in Fig EV2B–K). Staining of P0 and P15 brains of wild-type and mutant mice with antibodies against GFAP showed in both cases the presence of numerous $GFAP^+$ cells (Fig EV3). Interestingly, glial cells in hGFAP-SDHD mice had a radial glia-like phenotype, with long processes, which were not present in normal $GFAP^+$ cells (Fig EV3H, I, K and L). Histological analyses at an intermediate (P5) stage of development are shown in Fig EV4. We established that the amount of *SdhD* functional allele was clearly diminished in P15 hGFAP-SDHD mice in comparison with homo- or heterozygous normal littermates (Fig 1N). MCII activity in brain mitochondria of hGFAP-SDHD mice was also decreased to less than 30% of that in homozygous controls (Fig 1O), thus confirming the deletion of the *SdhD* gene in a significant proportion of brain cells. In accord with the morphological data, these biochemical differences were not observed when only the ventral parts of the brains were used for analysis (data not shown). *SdhD* mRNA levels and MCII activity were already decreased in newborn (P0) hGFAP-SDHD brains, indicating that ablation of the *SdhD* gene had taken place during embryonic life, as soon as the hGFAP promoter became active (see Fig EV1M and N). To ensure that the Cre-mediated loxP recombination had actually resulted in deletion of the *SdhD* alleles in $GFAP^+$ cells, we generated control and hGFAP-SDHD mouse lines that expressed the enhanced green fluorescent protein (EGFP) driven by the hGFAP promoter (see Materials and Methods). After dissociation, $GFAP^+$ cells were sorted from two different brain areas (cortex and striatum) (Fig 1P and Q). In both cases, the levels of *SdhD* mRNA were reduced to $< 20\%$ of the value in control mice (Fig 1R and S), thus demonstrating that the *SdhD* gene was ablated in $GFAP^+$ cells from hGFAP-SDHD mice. These findings suggest that brain NSCs, along with their progeny of neuroblasts and astrocytes generated before birth, appear to be little affected by mitochondrial dysfunction. However, neuronal maturation, a process that occurs in the perinatal period, seems to be highly dependent on proper mitochondrial oxidative metabolic function.

The extensive brain atrophy in hGFAP-SDHD mice is in fair agreement with previous lineage-specific tracing experiments showing that, during development, radial glia are stem cells from which many central neurons in the cortical and subcortical areas are derived [10]. Although these data, using Cre/loxP recombination of reporter genes, could be susceptible to misinterpretation due to the failure of reporter activity, our experiments, based on recombination of an intrinsic gene (*SdhD*) essential for cell homeostasis, fully confirm these results. Indeed, regional brain atrophy in the hGFAP-SDHD mice is almost superimposable on the distribution of labeled ($X\text{-}gal^+$) cells described in lineage tracing experiments using the same human GFAP promoter to drive Cre recombinase expression [10]. Relative preservation of ventral brain areas in hGFAP-SDHD animals can therefore be explained by the differential distribution of Cre-mediated recombination, which in hGFAP-Cre mice spares neural cells in this region.

Adult SVZ stem cells are preserved in SDHD-deficient mice, but survival of newly generated neurons and oligodendrocytes is impaired

Adult NSCs in the SVZ, which are considered to derive from radial glia, also have a $GFAP^+$ astrocyte-like phenotype [11]. We therefore investigated whether mitochondrial dysfunction influenced the maintenance, proliferation, and/or multipotency of these stem cells. Neurosphere assays of dispersed SVZ cells obtained from control and hGFAP-SDHD animals showed that the number of clonal colonies generated was the same for the two mouse strains (Fig 2A and B). Self-renewal capacity, as evidenced by the number of secondary

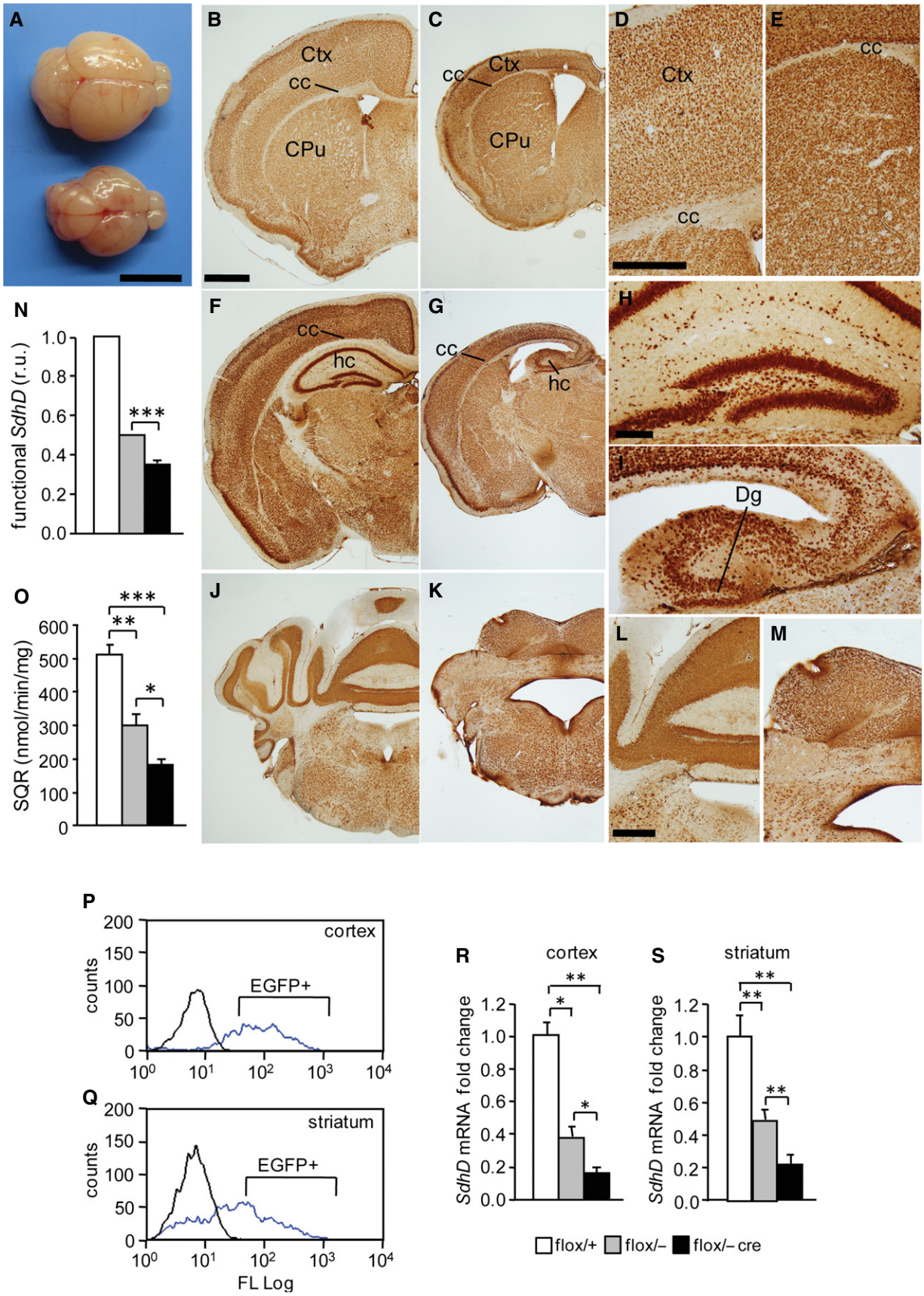

Figure 1.

Figure 1. Brain structures and mitochondrial complex II activity in wild-type and hGFAP-SDHD mice.

A Photographs of control (top) and hGFAP-SDHD (bottom) brains at P15. Scale bar: 5 mm.

B–M Brain sections of postnatal (P15) control (B, D, F, H, J, L) and hGFAP-SDHD (C, E, G, I, K, M) mice immunostained with NeuN antibody. Scale bars: 1 mm (B, C, F, G, J, K), 500 μm (D, E, H, I), and 200 μm (L, M). Ctx: cortex; cc: corpus callosum; CPu: caudate putamen; hc: hippocampus; Dg: dentate gyrus.

N Relative levels of functional *SdhD* allele in the entire brain (P15) as determined by qPCR of genomic DNA. r.u.: relative units (n = 4).

O Succinate–ubiquinone oxidoreductase (SQR) activity of mitochondria isolated from the entire brain (P15) (n = 6).

P, Q Representative profiles of sorted astrocytes from cortex and striatum of mice carrying the hGFAP-EGFP transgene (blue lines). Animals without the construct (black line) were used as blanks to determine the selection gates.

R, S Relative *SdhD* mRNA levels in sorted GFAP-expressing astrocytes from the cortex and striatum of control and hGFAP-SDHD mice.

Data information: Data are presented as mean ± SEM (n = 4–8). Statistical significance: *$P \leq 0.05$; **$P \leq 0.01$; ***$P \leq 0.001$. The ANOVA test with the appropriate *post hoc* analysis was applied. See also Figs EV1–EV4.

neurospheres, was also unaffected by the *SdhD* deletion (Fig EV5). These data suggest that SVZ stem cells are well preserved in hGFAP-SDHD mice with defective mitochondria. Nonetheless, the size of the primary (Fig 2A and C) and secondary (Fig EV5C) neurospheres was smaller in hGFAP-SDHD mice compared to controls (see below). Quantitative PCR analysis of *SdhD* mRNA from neurospheres confirmed the ablation of the *SdhD* gene in SVZ cells of genetically modified mice (Fig 2D). Furthermore, SVZ stem

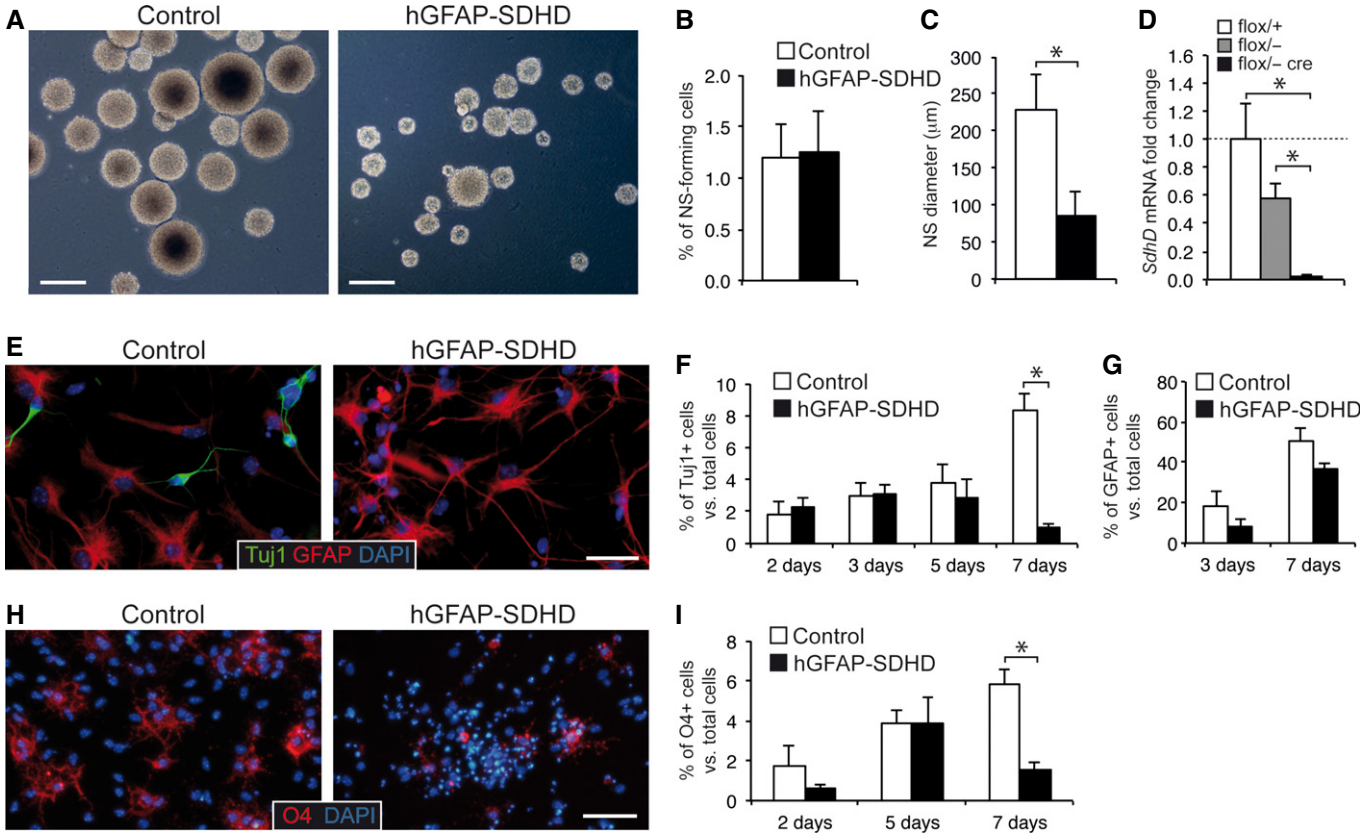

Figure 2. Effects of mitochondrial dysfunction on subventricular zone neural stem cells.

A Bright-field images of neurospheres obtained from SVZ neural stem cells of P15 control and hGFAP-SDHD mouse brains. Scale bars: 500 μm.

B, C Neurosphere (NS) forming efficiency (B) and core diameter (C) in cultures grown from SVZ of P15 control and hGFAP-SDHD mice (n = 6 cultures/mice for each genotype).

D Quantitative RT–PCR detection of *SdhD* expression levels in SVZ neurospheres of wild-type (flox/+) and mutant (flox/–, and flox/– cre) mice (n = 3–4 mice on each group).

E Immunofluorescence detection of the neuronal marker Tuj1 in SVZ neural stem cell-derived adherent cultures from P15 control or hGFAP-SDHD brains. Nuclei were counterstained with DAPI. Scale bar: 25 μm.

F Number of Tuj1$^+$ neurons generated in SVZ neural stem cell adherent cultures *in vitro* for several days (n = 8 cultures/mice for each genotype).

G Number of GFAP$^+$ astrocytes present in adherent cultures of SVZ neurospheres illustrating the resistance of glial cells to the loss of mitochondrial function (n = 5 independent cultures).

H Immunofluorescence detection of the oligodendrocyte marker O4 in SVZ neural stem cell-derived adherent cultures from P15 control or hGFAP-SDHD brains. Nuclei were counterstained with DAPI. Scale bar: 25 μm.

I Number of O4$^+$ neurons generated in SVZ neural stem cell adherent cultures *in vitro* for several days (n = 5–7 cultures/mice for each genotype). See also Fig EV5.

Data information: Data are presented as mean ± SEM. *$P \leq 0.05$. The two-tailed Student's t-test was applied.

cells from hGFAP-SDHD animals were able to differentiate into Tuj1$^+$ neurons *in vitro*; however, survival of these newly generated neurons was compromised (Fig 2E and F). In contrast, the differentiation and survival of astrocytes were practically unaltered in *SdhD*-defective neurospheres (Fig 2E and G). Survival of differentiated oligodendrocytes was also decreased in preparations from hGFAP-SDHD mice (Fig 2H and I). These observations provide direct experimental support for the notion that, as other progenitor cell types [5,6], central NSCs rely predominantly on anaerobic metabolism and thus can survive and maintain their normal function even after severe mitochondrial damage. However, maintenance of mature neurons and oligodendrocytes, but not GFAP$^+$ astrocytes, is absolutely dependent on a correctly functioning mitochondrial metabolism.

hGFAP-SDHD mice have normal PNS development but impaired carotid body neurogenesis

Despite the gross brain developmental alterations exhibited by the hGFAP-SDHD mice, they showed an apparently normal PNS. The morphology and number of neurons in the adrenal medulla, superior cervical ganglion (SCG), ENS, and dorsal root ganglia, all of which are derived from neural crest progenitor cells [12], were similar in P15 hGFAP-SDHD mice compared with controls (Fig 3A–H). We checked that, as in the CNS glia, GFAP$^+$ Schwann cells in peripheral nerves were also lacking the *SdhD* alleles, thereby demonstrating recombination of the floxed *SdhD* alleles in PNS structures (Fig 3I and J). Interestingly, ablation of the *SdhD* gene did not seem to compromise survival of these peripheral glial cells (Fig 3K), although extensive loss of TH$^+$ adrenal chromaffin cells and SCG neurons has been observed in previous studies with TH$^+$-specific *SdhD*-deficient (TH-SDHD) mice [18]. Quantitative PCR and histological analyses showed no differences in the SCG of hGFAP-SDHD and control mice (Fig EV6). A small, and non-significant, decrease in *SdhD* mRNA observed in the SCG of hGFAP-SDHD mice with respect to controls probably reflected *SdhD* deletion in the small population of GFAP$^+$ glial cells existing in this structure (Fig EV6A and B). Lack of hGFAP-Cre-dependent activity in peripheral neurons was further demonstrated *in vivo* using a LacZ reporter mice [16], which showed the absence of β-gal staining in TH$^+$ neurons from SCG (Fig EV6C and D). Taken together, these data suggest that NSCs giving rise to PNS neurons do not have the GFAP$^+$ glial origin that is characteristic of brain NSCs. An exception to this general rule appears to be the CB, which in newborn (P0) hGFAP-SDHD mice had similar size to that of control animals (Fig 4A–C). However, the normal postnatal increase in TH$^+$ glomus cell number and the volume of TH$^+$ CB parenchyma observed in controls were abolished in hGFAP-SDHD mice (Fig 4A–C). Despite the decrease in CB neuron-like glomus cell number, the population of CB stem cells in the hGFAP-SDHD mice remained unaltered as judged by the ability of dispersed CB stem cells to form growing neurospheres (Fig 4D–F). These observations indicate that unlike other structures in the PNS, postnatal development of the CB depends on glia-like GFAP$^+$ stem cells that are also resistant to mitochondrial dysfunction. A population of these glia-like cells remains dormant in the adult CB and sustains its adaptive growth upon exposure to chronic hypoxia [16,17]. Other stem cells in the adult PNS do not seem to contribute to the physiological homeostasis of the specific tissues where they are located [14,15]. Therefore, NSCs of glial lineage that reside in the adult CB constitute a neurogenic niche of similar characteristics to those existing in the adult brain and confer upon the CB the anatomical and functional plasticity required for acclimatization to hypoxia [17]. The expression of GFAP in brain and CB neural stem cells could in fact be the manifestation of a quiescent state in these cells that is necessary to maintain their capacity to generate neurons in adulthood.

Mitochondria and neural stem cell proliferation and differentiation

We have shown that low reliance on mitochondrial oxidative phosphorylation seems to be a common generic feature of NSCs during development and in the adult niches. Nonetheless, the way different stem cell classes achieve a homeostatic anaerobic metabolism may be variable. Several groups have reported a smaller number of mitochondria and modifications of their shape in multipotent HSCs in comparison to more-committed bone marrow progenitors [2]. Moreover, the high glycolytic flux of quiescent HSCs residing in hypoxic niches seems to rely on the upregulation of hypoxia-inducible transcription factors (particularly HIF-1α) and the subsequent induction of glycolytic enzymes and pyruvate dehydrogenase kinase to blunt pyruvate-dependent oxidative phosphorylation [5,6,19]. However, it has been reported that although stabilization of HIF-1α and HIF-2α is necessary to initiate the metabolic switch in the early stages of the reprogramming of human cells to iPSCs, the stabilization of HIF-2α during latter stages represses reprogramming [9]. HIF-1α-deficient NSCs have normal mitochondria although they are resistant to hypoxia and have high glycolytic activity [20]. Recently, we showed that maintenance and clonal growth of CB stem cells *in vitro* is unaffected by a broad range of O_2 tensions [17]. This insensitivity to O_2 tension is also observed in neurosphere cultures of adult SVZ stem cells [21] as well as in embryonic stem cells [3]. Although we have observed that survival of central (SVZ) and peripheral (CB) neural stem cells

Figure 3. Normal development and survival of peripheral neurons in hGFAP-SDHD mice.

A–H Immunofluorescence detection of neuronal markers TH (A, C) and HuC/D (E, G) in the adrenal medulla (A), superior cervical ganglion (C), enteric ganglia at the level of the distal small intestine (E), and dorsal root ganglion (G) of P15 control and hGFAP-SDHD mice. Scale bars: 200 μm (A, C), 100 μm (E, G). Cell number in adrenal medulla (B), superior cervical ganglion (D), enteric ganglia (F), and dorsal root ganglion (H) in the same animal models. Data are presented as mean ± SEM (n = 4–7 per group).

I Immunofluorescence detection of GFAP expression in cross sections of peripheral sciatic nerve illustrating the normal shape of Schwann cells forming myelin sheaths in P15 control and hGFAP-SDHD mice. Scale bar: 50 μm.

J Results of quantitative RT–PCR to detect *SdhD* expression in the peripheral nerves of wild-type (flox/+) and mutant (flox/−, and flox/− cre) mice. Data are presented as mean ± SEM (n = 3 flox/+, n = 6 flox/−, and n = 8 flox/− cre mice). Statistical significance: *$P \leq 0.05$; **$P \leq 0.01$. The two-tailed Student's t-test was applied.

K Number of myelin sheaths per unit area in sciatic nerves of P15 control and mutant mice. Data are presented as mean ± SEM (n = 4 mice for each genotype). See also Fig EV6.

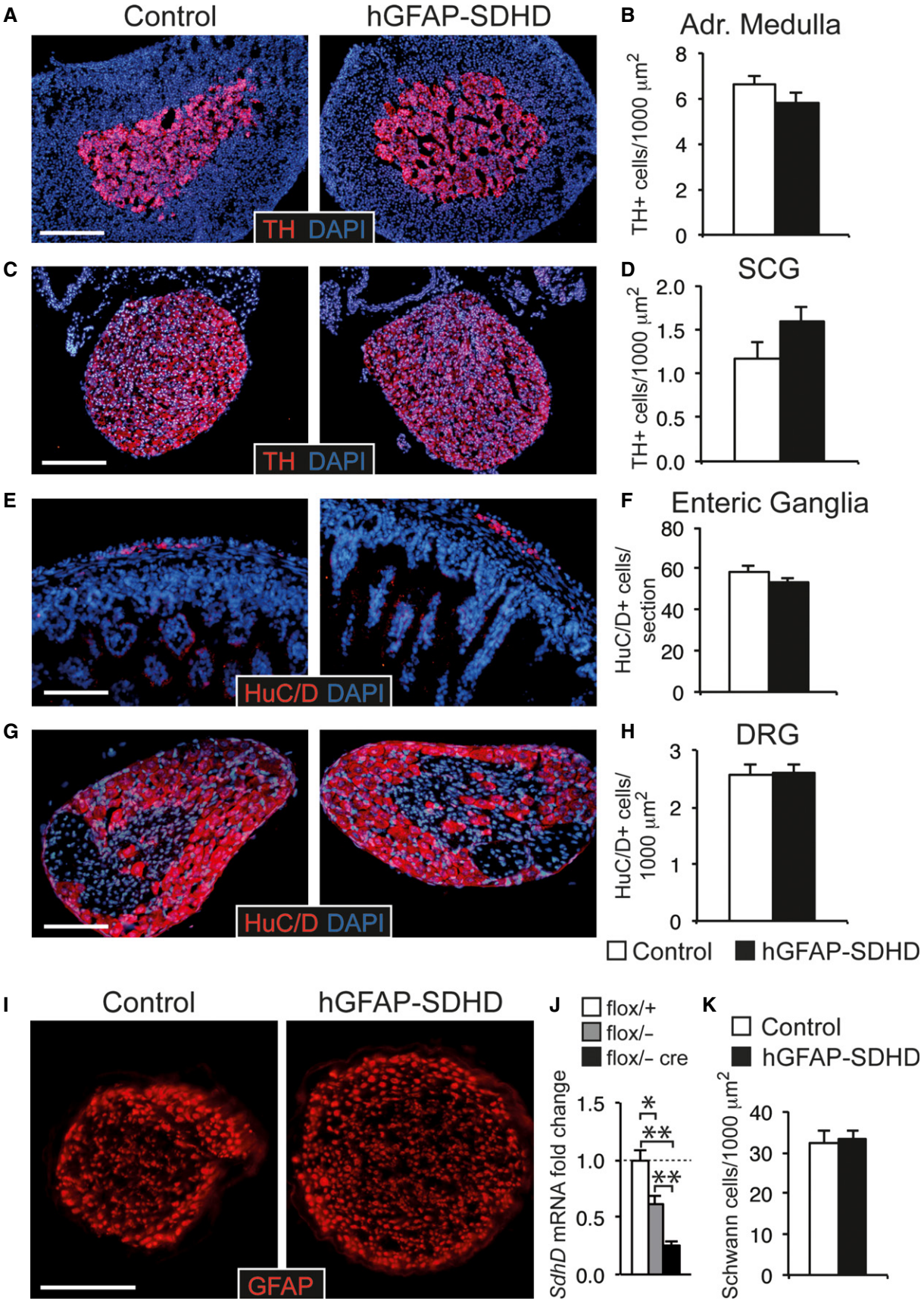

Figure 3.

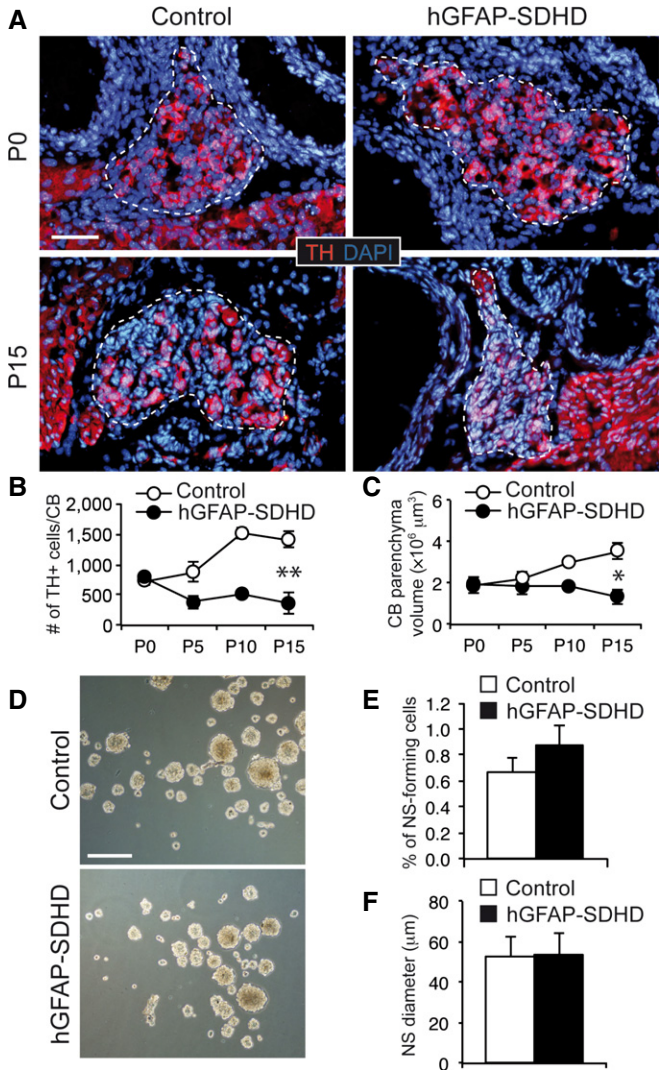

Figure 4. Impairment of carotid body postnatal maturation with maintenance of adult stem cells in hGFAP-SDHD mice.

A Immunofluorescence detection of TH expression in newborn (P0) and P15 wild-type (control) and hGFAP-SDHD mouse carotid body (CB). Boundaries of the CB parenchyma are indicated by the dotted lines. Scale bar: 50 µm.

B, C Number of TH^+ cells (B) and size (C) per CB at different ages in control and hGFAP-SDHD mice. Data are presented as mean ± SEM (n = 3–5 mice in each group). *$P \leq 0.05$; **$P \leq 0.01$. The two-tailed Student's t-test was applied.

D Bright-field images of CB neurospheres obtained from control and mutant mice at P15. Scale bar: 200 µm.

E, F Neurosphere forming efficiency (E) and diameter (F) of floating cultures of dispersed CB cells from P15 control and hGFAP-SDHD mice. Data are presented as mean ± SEM (n = 6 cultures/mice for each genotype).

is not affected by mitochondrial dysfunction, proliferation of SVZ progenitors (as estimated by the size of neurosphere cores) was reduced in preparations from hGFAP-SDHD mice. This could indicate that the high rate of *in vitro* proliferation of central progenitors (in comparison with progenitors in CB neurospheres) makes them partially dependent on energy obtained by oxidative phosphorylation. Taken together, these data suggest that a high glycolytic flux and resistance to mitochondrial dysfunction are characteristic properties of stem cells regardless of O_2 tension levels. Therefore, besides the hypoxic stabilization of HIF, other intrinsic mechanisms and/or niche factors might contribute to the anaerobic metabolic state associated with the maintenance of NSC multipotency.

Although mitochondrial dysfunction was not seen to alter NSC maintenance and multipotency in the present study, it exerted a marked effect on the survival of their central and peripheral neural progeny. Defective mitochondrial metabolism seemed to impair radial glial cell differentiation, as in P15 animals they appeared in a state typical of the prenatal brain. However, these mutated radial glia cells were able to differentiate into neurons, oligodendrocytes, and astrocytes. Brains from neonatal wild-type and hGFAP-SDHD mice showed similar sizes, structures, and $NeuN^+$ cell densities, suggesting that neuronal maturation occurring during the first postnatal weeks rather than neuroblast differentiation is the process that was actually compromised in mitochondria-defective animals. On the other hand, we observed the appearance of neurons and oligodendrocytes in differentiation assays of SVZ stem cells from hGFAP-SDHD mice, although these cells did not survive longer than a few days. Understanding the role of mitochondria on stemness and the switching from quiescence to activity in stem cells located in the different niches may help in the development of new therapeutic strategies against cancer stem cells.

Materials and Methods

Animals

The hGFAP-SDHD strain with $SdhD^{flox/-}$ hGFAP-CRE genotype was obtained by breeding the previously reported *SdhD*-flox mouse strain [18] with a mouse line expressing Cre under control of the human GFAP promoter, which is active in mouse radial glia [10,22]. Littermates with $SdhD^{flox/+}$ and $SdhD^{flox/-}$ genotypes lacking CRE recombinase are referred to as flox/+ and flox/−, respectively. Where indicated, results from both genotypes were pooled and assigned to a control group since no differences between them were found for the phenotypes tested. Routine genotyping was performed for the *SdhD* alleles and the CRE gene by PCR as previously reported [10,22]. hGFAP-SDHD mice carrying the enhanced green fluorescence protein (EGFP) under control of the human GFAP promoter were obtained by breeding with the hGFAP-EGFP strain [23]. Mice were housed under temperature-controlled conditions (22°C) on a 12-h light/dark cycle, and provided with food and water *ad libitum*. Mice were housed and treated according to the animal care guidelines of the European Community Council (86/609/EEC), as well as institutional guidelines approved by the ethics committee of the Hospital Universitario Virgen del Rocio and the University of Seville (see Appendix Supplementary Materials and Methods).

Histochemistry and immunocytochemistry

For detection of NeuN, GFAP, TH, O4, HuC/D, Tuj1, and β-gal in tissue sections, neurospheres, and dissociated cells, we used standard staining procedures. Specific details are given in the Appendix Supplementary Materials and Methods.

Tissue dissociation, cell sorting, and neurosphere assays

Dissociated cells were obtained from brain and CB tissue following standard procedures. Cell sorting and the generation of SVZ and CB neurospheres were carried out as indicated previously [16]. See Appendix Supplementary Materials and Methods.

SdhD DNA and mRNA analyses

DNA and RNA analyses were performed as described previously [18]. See Appendix Supplementary Materials and Methods.

Mitochondria isolation and complex II activity

Mitochondrial complex II activity was determined according to Piruat *et al* [24] with slight modifications. See Appendix Supplementary Materials and Methods.

Statistics

Data are presented as mean ± standard error (SEM). Statistical significance was assessed by ANOVA with appropriate *post hoc* analysis. For paired groups, either a two-tailed Student's *t*-test with a Levene test for homogeneity of variances in the case of normal distribution, or the nonparametric Mann–Whitney *U*-test in the case of non-normal distributions, was applied. Normal distribution was assessed by Shapiro–Wilk test. PASW18 software was used for statistical analysis.

Expanded View for this article is available online:
http://embor.embopress.org

Acknowledgements
This research is supported by grants from the Botín Foundation (JL-B), the Spanish Ministry of Science and Innovation SAF program (JL-B, RP and JIP), the European Research Council (RP and JL-B), and the Junta de Andalucía (JIP). We thank Alberto Castejón, Valentina Annese, and María José Castro for technical assistance.

Author contributions
BD-C, RP, PG-F, VS, RD, and JIP performed experiments. BD-C, RP, JIP, and JL-B designed experiments and contributed to generate a draft of the manuscript. JL-B coordinated the project.

Conflict of interest
The authors declare that they have no conflict of interest.

References

1. Suda T, Takubo K, Semenza GL (2011) Metabolic regulation of hematopoietic stem cells in the hypoxic niche. *Cell Stem Cell* 9: 298 – 310
2. Xu X, Duan S, Yi F, Ocampo A, Liu GH, Izpisua Belmonte JC (2013) Mitochondrial regulation in pluripotent stem cells. *Cell Metab* 18: 325 – 332
3. Ezashi T, Das P, Roberts RM (2005) Low O_2 tensions and the prevention of differentiation of hES cells. *Proc Natl Acad Sci USA* 102: 4783 – 4788
4. Mohyeldin A, Garzon-Muvdi T, Quinones-Hinojosa A (2010) Oxygen in stem cell biology: a critical component of the stem cell niche. *Cell Stem Cell* 7: 150 – 161
5. Simsek T, Kocabas F, Zheng J, Deberardinis RJ, Mahmoud AI, Olson EN, Schneider JW, Zhang CC, Sadek HA (2010) The distinct metabolic profile of hematopoietic stem cells reflects their location in a hypoxic niche. *Cell Stem Cell* 7: 380 – 390
6. Takubo K, Nagamatsu G, Kobayashi CI, Nakamura-Ishizu A, Kobayashi H, Ikeda E, Goda N, Rahimi Y, Johnson RS, Soga T *et al* (2013) Regulation of glycolysis by Pdk functions as a metabolic checkpoint for cell cycle quiescence in hematopoietic stem cells. *Cell Stem Cell* 12: 49 – 61
7. Folmes CD, Nelson TJ, Dzeja PP, Terzic A (2012) Energy metabolism plasticity enables stemness programs. *Ann N Y Acad Sci* 1254: 82 – 89
8. Inoue S, Noda S, Kashima K, Nakada K, Hayashi J, Miyoshi H (2010) Mitochondrial respiration defects modulate differentiation but not proliferation of hematopoietic stem and progenitor cells. *FEBS Lett* 584: 3402 – 3409
9. Mathieu J, Zhou W, Xing Y, Sperber H, Ferreccio A, Agoston Z, Kuppusamy KT, Moon RT, Ruohola-Baker H (2014) Hypoxia-inducible factors have distinct and stage-specific roles during reprogramming of human cells to pluripotency. *Cell Stem Cell* 14: 592 – 605
10. Malatesta P, Hack MA, Hartfuss E, Kettenmann H, Klinkert W, Kirchhoff F, Gotz M (2003) Neuronal or glial progeny: regional differences in radial glia fate. *Neuron* 37: 751 – 764
11. Kriegstein A, Alvarez-Buylla A (2009) The glial nature of embryonic and adult neural stem cells. *Annu Rev Neurosci* 32: 149 – 184
12. Le Douarin N, Dulac C, Dupin E, Cameron-Curry P (1991) Glial cell lineages in the neural crest. *Glia* 4: 175 – 184
13. Morrison SJ, White PM, Zock C, Anderson DJ (1999) Prospective identification, isolation by flow cytometry, and in vivo self-renewal of multipotent mammalian neural crest stem cells. *Cell* 96: 737 – 749
14. Joseph NM, He S, Quintana E, Kim YG, Nunez G, Morrison SJ (2011) Enteric glia are multipotent in culture but primarily form glia in the adult rodent gut. *J Clin Invest* 121: 3398 – 3411
15. Laranjeira C, Sandgren K, Kessaris N, Richardson W, Potocnik A, Vanden Berghe P, Pachnis V (2011) Glial cells in the mouse enteric nervous system can undergo neurogenesis in response to injury. *J Clin Invest* 121: 3412 – 3424
16. Pardal R, Ortega-Saenz P, Duran R, Lopez-Barneo J (2007) Glia-like stem cells sustain physiologic neurogenesis in the adult mammalian carotid body. *Cell* 131: 364 – 377
17. Platero-Luengo A, Gonzalez-Granero S, Duran R, Diaz-Castro B, Piruat JI, Garcia-Verdugo JM, Pardal R, Lopez-Barneo J (2014) An O_2-sensitive glomus cell-stem cell synapse induces carotid body growth in chronic hypoxia. *Cell* 156: 291 – 303
18. Diaz-Castro B, Pintado CO, Garcia-Flores P, Lopez-Barneo J, Piruat JI (2012) Differential impairment of catecholaminergic cell maturation and survival by genetic mitochondrial complex II dysfunction. *Mol Cell Biol* 32: 3347 – 3357
19. Romero-Moya D, Bueno C, Montes R, Navarro-Montero O, Iborra FJ, Lopez LC, Martin M, Menendez P (2013) Cord blood-derived $CD34^+$ hematopoietic cells with low mitochondrial mass are enriched in hematopoietic repopulating stem cell function. *Haematologica* 98: 1022 – 1029
20. Candelario KM, Shuttleworth CW, Cunningham LA (2013) Neural stem/progenitor cells display a low requirement for oxidative metabolism independent of hypoxia inducible factor-1alpha expression. *J Neurochem* 125: 420 – 429

21. d'Anglemont de Tassigny X., Sirerol-Piquer M.S., Gómez-Pinedo U., Pardal R., Bonilla S., Capilla-Gonzalez V., López-López I., De la Torre-Laviana F.J., García-Verdugo J.M., López-Barneo J. (2015). Resistance of subventricular neural stem cells to chronic hypoxemia despite structural disorganization of the germinal center and impairment of neuronal and oligodendrocyte survival. *Hypoxia* 3: 15 – 33.
22. Zhuo L, Theis M, Alvarez-Maya I, Brenner M, Willecke K, Messing A (2001) hGFAP-cre transgenic mice for manipulation of glial and neuronal function in vivo. *Genesis* 31: 85 – 94
23. Nolte C, Matyash M, Pivneva T, Schipke CG, Ohlemeyer C, Hanisch UK, Kirchhoff F, Kettenmann H (2001) GFAP promoter-controlled EGFP-expressing transgenic mice: a tool to visualize astrocytes and astrogliosis in living brain tissue. *Glia* 33: 72 – 86
24. Piruat JI, Pintado CO, Ortega-Saenz P, Roche M, Lopez-Barneo J (2004) The mitochondrial SDHD gene is required for early embryogenesis, and its partial deficiency results in persistent carotid body glomus cell activation with full responsiveness to hypoxia. *Mol Cell Biol* 24: 10933 – 10940